CORRIGENDUM

ROBERT C. J. WILLS,[a] KYLE C. ARMOUR,[a,b] DAVID S. BATTISTI,[a] CRISTIAN PROISTOSESCU,[c,d] AND LUKE A. PARSONS[e]

[a] *Department of Atmospheric Sciences, University of Washington, Seattle, Washington*
[b] *School of Oceanography, University of Washington, Seattle, Washington*
[c] *Department of Atmospheric Sciences, University of Illinois Urbana–Champaign, Urbana, Illinois*
[d] *Department of Earth Science and Environmental Change, University of Illinois Urbana–Champaign, Urbana, Illinois*
[e] *Nicholas School of the Environment, Duke University, Durham, North Carolina*

(Manuscript received 24 March 2023, in final form 13 April 2023, accepted 13 April 2023)

There was an error in the processing of the sea surface temperature (SST) model output used in Wills et al. (2021). The SST data from the CMIP6 preindustrial control (piControl) simulations used to compute the low-frequency patterns (LFPs) were not quadratically detrended as intended, which resulted in the low-frequency components (LFCs) containing trends associated with drift in the piControl simulations. All other variables were quadratically detrended, which resulted in reduced values of the covariances between the LFCs and other fields compared to updated results with all fields detrended. Quadratically detrending all model output before analysis gives qualitatively similar results with minor quantitative differences. The overall conclusions of the paper are unaffected. Nevertheless, we have included updated versions of the seven figures that were affected by this error (Figs. 1, 2, 3, 6, 7, 8, and 11), along with an updated Table 1.

We also highlight a few of the quantitative differences in our updated results. Most notably, the coherence of LFC-1 with global-mean surface temperature (GMST) at 40–200-yr time scales increased from 0.45–0.5 in Wills et al. (2021) to 0.65–0.7 in our updated results (Fig. 2), indicating that LFC-1 plays an even larger role in the multidecadal variability of GMST in CMIP6 piControl simulations than our previous results suggested. Correspondingly, the maximum impact of LFC-1 on decadal-running-mean GMST anomalies increased from 0.47° to 0.55°C. Some of this change results from a redistribution of variability between LFC-1 and LFC-2, and the impact of LFC-2 on decadal-running-mean GMST is reduced from 0.29° to 0.25°C in our updated results. With these updated numbers, LFCs 1 and 2 explain 51% and 11% of the variance in decadal-running-mean GMST, respectively. Changes in the covariances between the leading LFCs and GMST also influence the diagnosed global radiative feedbacks (updated Table 1) and lead to small changes in the impacts of LFCs 1 and 2 on effective climate sensitivity (EffCS; Fig. 11), with a slightly greater impact of LFC-1 and a slightly reduced impact of LFC-2 relative to Wills et al. (2021).

REFERENCE

Wills, R. C. J., K. C. Armour, D. S. Battisti, C. Proistosescu, and L. A. Parsons, 2021: Slow modes of global temperature variability and their impact on climate sensitivity estimates. *J. Climate*, **34**, 8717–8738, https://doi.org/10.1175/JCLI-D-20-1013.1.

Corresponding author: Robert C. Jnglin Wills, r.jnglinwills@usys.ethz.ch

DOI: 10.1175/JCLI-D-22-0308.1

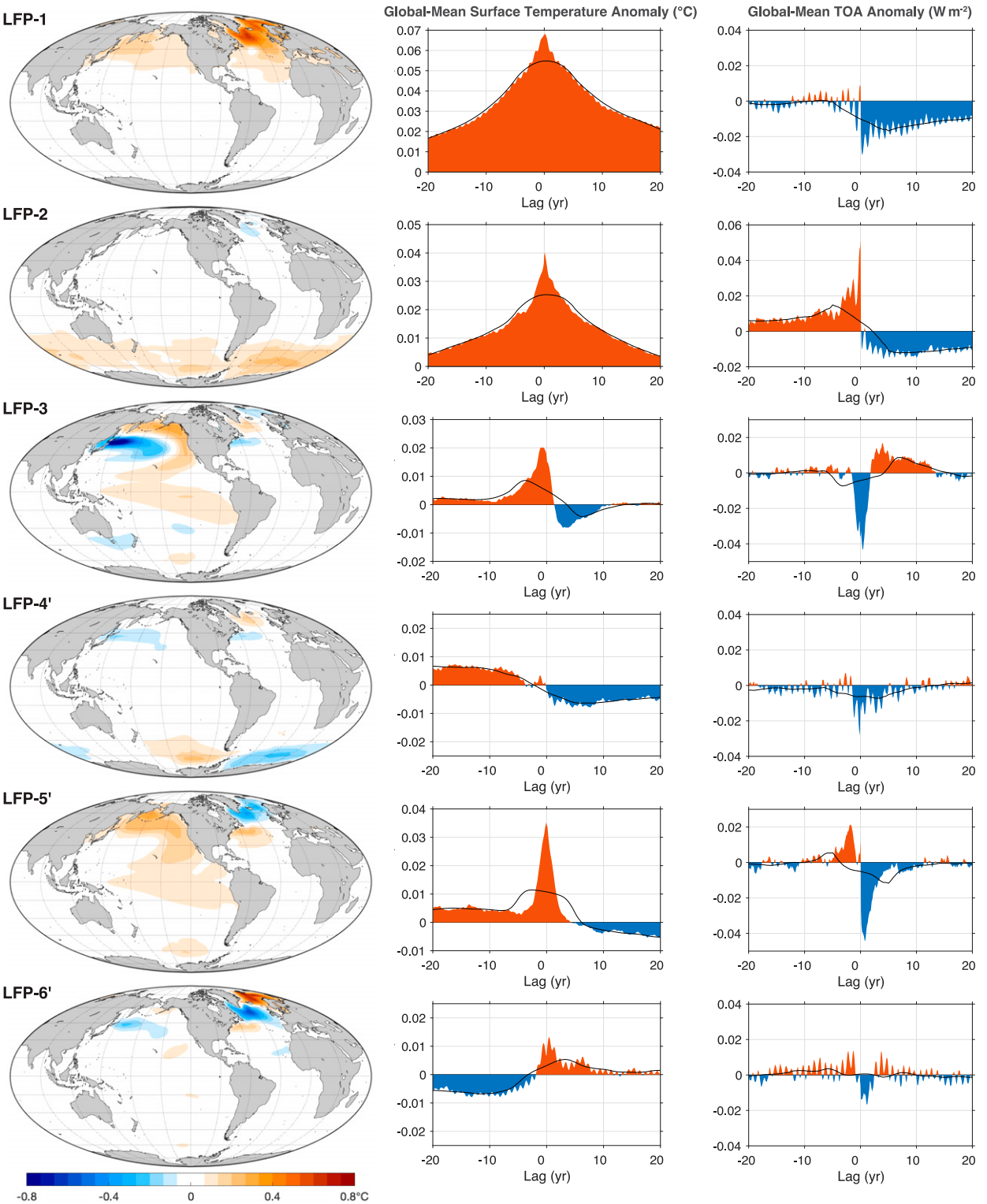

FIG. 1. LFPs 1–6 of CMIP6 piControl simulations and their impacts on GMST and global-mean top-of-atmosphere (TOA) radiation (GMTOA): (left) the SST anomaly pattern (LFP), (center) the lead–lag regression of monthly GMST anomalies on the associated LFCs, and (right) the lead–lag regression of monthly GMTOA anomalies on the associated LFCs; negative values indicate a loss of energy to space. Black lines show the same lead–lag regressions, but for the 10-yr running mean GMST and GMTOA anomalies. Positive lags indicate anomalies that occur after the maximum anomaly in the LFC. All calculations are averaged over 35 CMIP6 models. A secondary rotation has been applied to LFPs 4–6 to localize them within ocean basins, as described in section 2b of Wills et al. (2021).

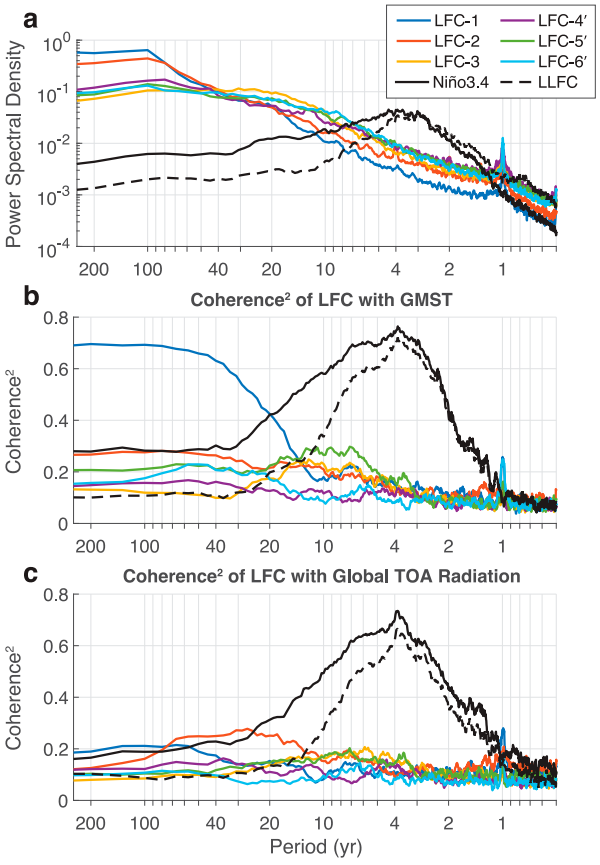

FIG. 2. (a) Power spectral density of the LFCs. (b) Squared coherence between the LFCs and GMST. (c) Squared coherence between the LFCs and GMTOA. All panels also show Niño-3.4 and the least-low-frequency component (LLFC) for comparison. The LLFC is strongly correlated with Niño-3.4 and is discussed in more detail in the text of Wills et al. (2021). All calculations are averaged over 35 CMIP6 piControl simulations.

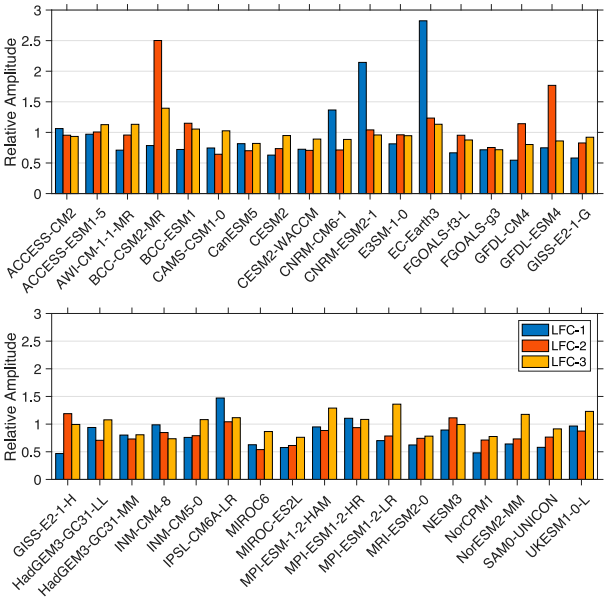

FIG. 3. Amplitude (standard deviation) of the six leading LFCs in each of the 35 CMIP6 piControl simulations, normalized by their amplitude in the multimodel composite.

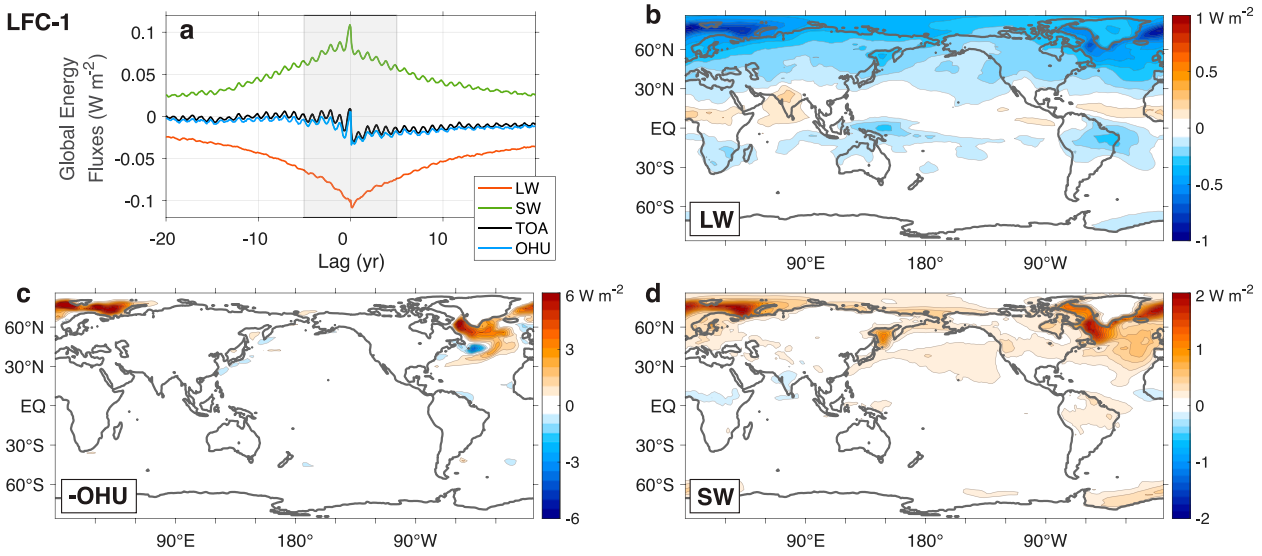

FIG. 6. Decadal-mean impact of the Atlantic multidecadal variability–like LFC-1 on the global energy budget. (a) Lead–lag regression of net incoming longwave radiation at TOA (LW), net incoming shortwave radiation at TOA (SW), net incoming radiation at TOA, and net ocean heat uptake (OHU) on LFC-1. Positive TOA flux anomalies correspond to a net energy input to the Earth system. Lag times indicate anomalies that lag LFC-1. Also shown are maps of 10-yr running-mean anomalies in (b) LW, (c) −OHU, and (d) SW associated with a 1-standard-deviation anomaly in LFC-1. The gray shading in (a) shows the averaging period used in (b)–(d). All calculations are averaged over 35 CMIP6 models.

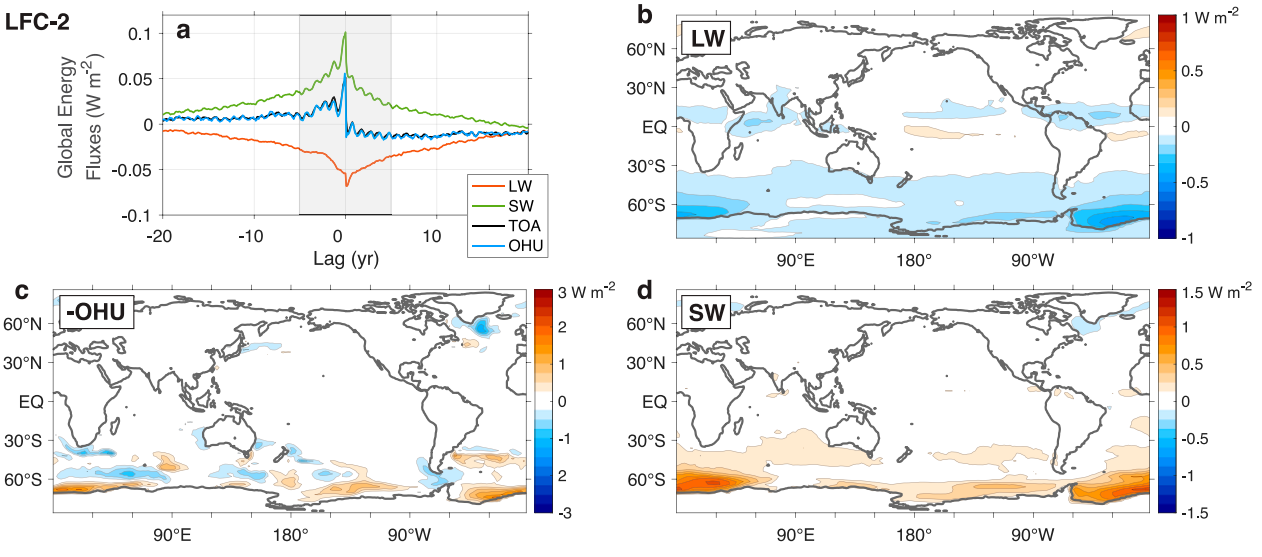

FIG. 7. As in Fig. 6, but for decadal-mean impact of LFC-2 (Southern Ocean multidecadal variability) on the global energy budget.

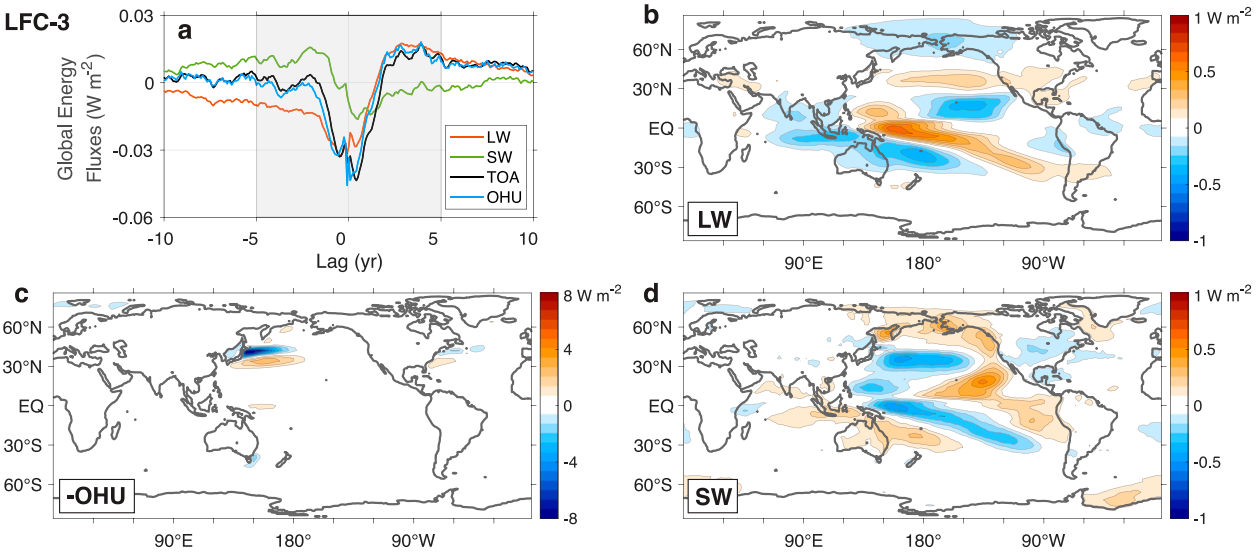

FIG. 8. As in Fig. 6, but for decadal-mean impact of the Pacific decadal variability–like LFC-3 on the global energy budget.

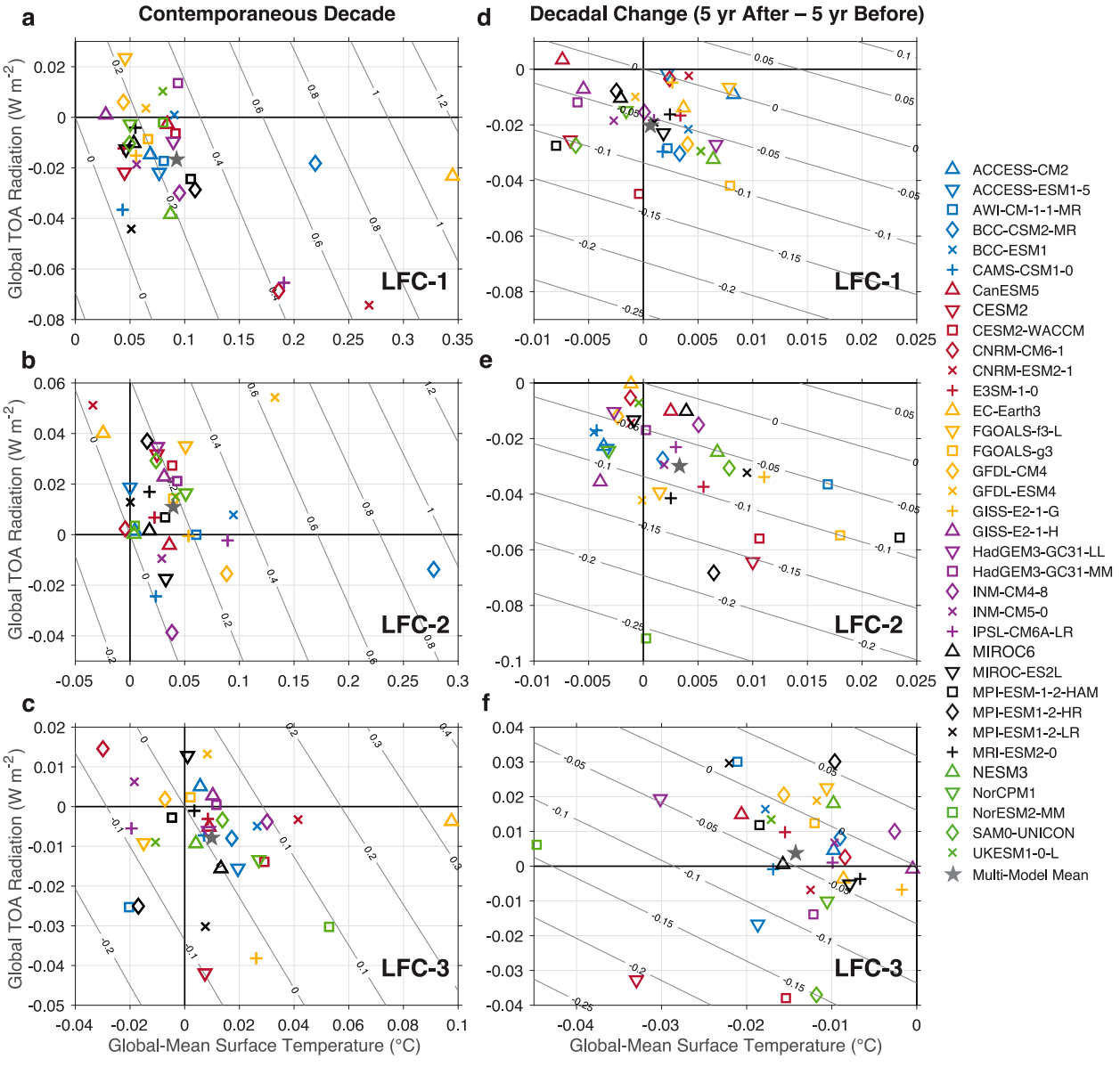

FIG. 11. Scatterplots of the lag-0 (contemporaneous) impact of a 2-standard-deviation anomaly in (a) LFC-1, (b) LFC-2, and (c) LFC-3 on 10-yr running-mean GMST (x axis) and 10-yr running-mean GMTOA (y axis) for all 35 of the CMIP6 piControl simulations. Also shown is the change in GMST (x axis) and GMTOA (y axis) between the 5 years before and 5 years after a 1-standard-deviation anomaly in (d) LFC-1, (e) LFC-2, and (f) LFC-3. Diagonal lines show the corresponding anomaly in effective climate sensitivity (EffCS) if these GMST and GMTOA anomalies are superimposed on a forced change of 1°C and 1.14 W m^{-2} (corresponding to an EffCS$_{\text{forced}}$ of 3.5°C).

TABLE 1. Multimodel median statistics of decadal GMST and GMTOA variability. The std dev column gives the standard deviation of each quantity. The LFC-1, LFC-2, LFC-3, LLFC, and Niño-3.4 columns give the lag-5 covariance of the corresponding quantity with each of these indices (i.e., the anomaly in the decade following the maximum in each index, in units of the corresponding quantity per standard deviation). The global climate feedback is calculated as the 10-yr running-mean GMTOA anomaly divided by the 10-yr running-mean GMST anomaly. The lag-5 covariance is used because of intermodel differences in the sign of some GMST and GMTOA anomalies at lag-0 [see section 5 of Wills et al. (2021)].

	Std dev	LFC-1	LFC-2	LFC-3	LLFC	Niño-3.4
10-yr running-mean GMST (°C)	0.077	0.047	0.021	−0.003	0.003	0.005
10-yr running-mean GMTOA (W m^{-2})	0.070	−0.017	−0.011	0.003	−0.011	−0.017
Global climate feedback (W m^{-2} K^{-1})	−0.90	−0.35	−0.52	−1.03	−2.88	−3.16